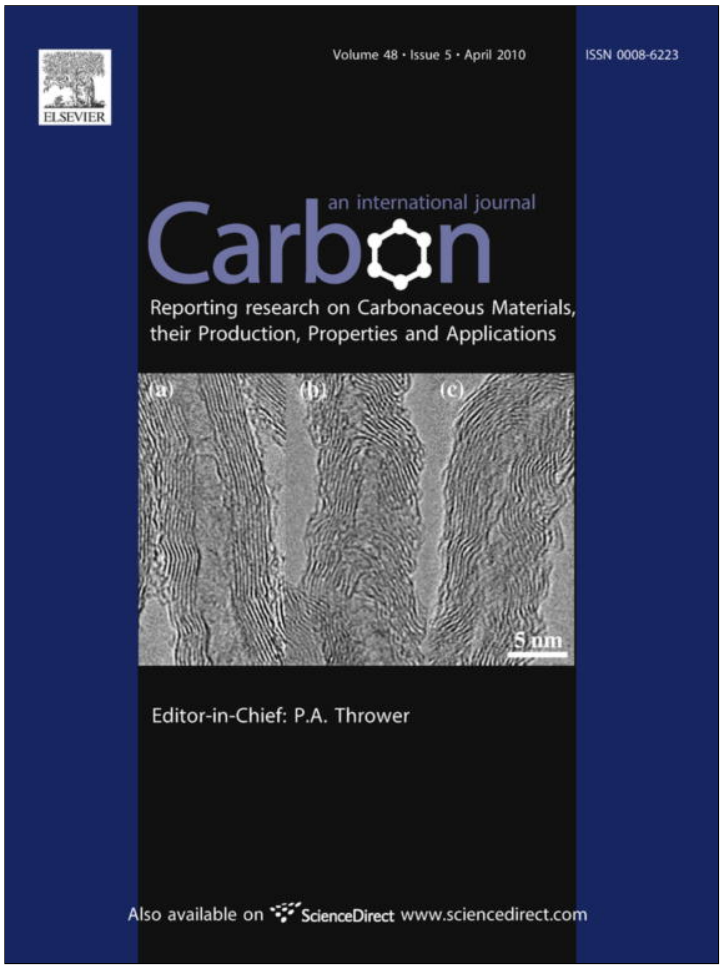

CARBON 48 (2010) 1362–1368

available at www.sciencedirect.com

ScienceDirect

journal homepage: www.elsevier.com/locate/carbon

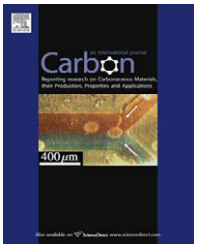

Field emission from a large area of vertically-aligned carbon nanofibers with nanoscale tips and controlled spatial geometry

Jia Yun [a], *Rui Wang* [b], *W.K. Choi* [a,b,*], *J.T.L. Thong* [a,b], *C.V. Thompson* [a,c], *Mei Zhu* [b], *Y.L. Foo* [d], *M.H. Hong* [b]

[a] *Advanced Materials for Micro- and Nano-Systems, Singapore-MIT Alliance, Singapore 117576, Singapore*
[b] *Department of Electrical and Computer Engineering, National University of Singapore, Singapore 117576, Singapore*
[c] *Department of Materials Science and Engineering, Massachusetts Institute of Technology, MA 02139, USA*
[d] *Institute of Materials Research and Engineering, ASTAR, Singapore 17602, Singapore*

ARTICLE INFO

Article history:
Received 24 August 2009
Accepted 8 December 2009
Available online 13 January 2010

ABSTRACT

A cost-effective method was used to fabricate large area (e.g. $2.5 \times 2.5\ cm^2$ for a pitch of 0.5 μm) nanometer scale pyramid arrays with precise and controllable location, spacing and size by interference lithography. Using this method a large-area of vertically-aligned carbon nanofibers (VACNFs) with different interfiber-distance-to-fiber-height ratios and fiber aspect ratios were synthesised. Very sharp tipped VACNFs were obtained and their field emission properties were measured and are compared to results in the literature. We find that the field emission performance of VACNF arrays is optimized when the interfiber-distance-to-fiber-height ratio is equal to 1, in line with some experimental findings but different from some predictions.

1. Introduction

Carbon nanotubes (CNTs) are considered to be promising candidates for field emission display applications, due to their good electrical and thermal properties [1], mechanical strength [2] and large height-to-radius ratio. Of the various chemical vapor deposition techniques used for the synthesis of CNTs, the plasma enhanced chemical vapor deposition (PECVD) technique is most widely used to grow large area vertically-aligned carbon nanotubes (VACNTs). It should be noted, however, that the CNTs synthesized by this method are generally defective, and these tubes are therefore sometimes referred to as carbon nanofibers (CNFs) [3].

There are quite a few experimental reports on the characterization of field emission properties of CNTs and CNFs. In these studies, CNTs or CNFs with relatively good control of tube or fiber geometry, location, and density were achieved using different catalyst patterning methods. These catalyst patterning techniques include: electron beam lithography (EBL) [4], nano sphere lithography (NSL) [5], nano imprinting lithography (NIL) [6] and the use of porous anodized aluminum oxide templates (AAO) [7,8]. Among these techniques, some provide very good control of catalyst geometry and location, but are costly and produce small area of device coverage (e.g. EBL). Others provide relatively large areas of device coverage area but suffer from restrictions on the catalyst geometry and location (e.g. NSL, AAO) or the need for fairly complicated processes to change geometry parameters (e.g. new masks for different spacings in the case of NIL).

* *Corresponding author:* Address: Department of Electrical and Computer Engineering, National University of Singapore, Singapore 117576, Singapore. Fax: +65 6779 1103.
E-mail address: elechoi@nus.edu.sg (W.K. Choi).
0008-6223/$ - see front matter
doi:10.1016/j.carbon.2009.12.026

On the theoretical side, Nilsson et al. [9] have reported on the influence of the distance between adjacent CNTs predicts that the "screening effect" can significantly deteriorate field emission characteristics of CNT arrays. This study had been widely cited by researchers working in this field. Nilsson et al.'s theoretical study was based on a two-dimensional simulation of thin (2 nm in radius) CNTs, and arrived at a conclusion that the optimum field emission performance could be achieved at a ratio of intertube distance (D) to tube length (l) equal to two. These conclusions were found to be at variance with experimental studies [7,8], probably due to (i) the prediction was based on a two-dimensional electrostatic simulation of CNT/CNF arrays (a line of emitters) while experimental results were obtained from three-dimensional arrays, (ii) patterned CNTs or CNFs in practice possess a tip radius much larger than 2 nm. Recently, a three-dimensional simulation study on field emission from CNTs found that the best field emission enhancement require a ratio of D/l equal to three [10].

To resolve all these discrepancies, we made use of a novel templating technique to control the size of Ni catalysts with a fixed separation and controlled the length of CNFs such that a systematic study on the influences of (a) interfiber-distance-to-fiber-height ratio (D/l), (Γ), and (b) the fiber aspect ratio (tube length over tube radius, l/r), (α), on the field emission characteristics of CNFs could be carried out.

2. Experimental

2.1. Ni catalyst patterning

To pattern the catalyst, we used a technique reported earlier that combines top-down and bottom-up approaches to provide precise in situ production and placement of metallic nanoparticles on silicon surface [11]. The top-down component of this method uses interference lithography (IL) [12], while the bottom-up process involves agglomeration (dewetting) of solid metallic thin films (AF) [13]. This method, denoted here as IL–AF, can position metal nanoparticles at predetermined locations on the silicon surface and, further, can accurately control the size of the nanoparticles. In the present work, we adopted this idea with slight improvements. Using this method, we prepared CNFs with different Γ and α values in order to investigate the *screening effect* and the *fiber aspect ratio* on the field emission performance of CNFs.

Fig. 1 outlines the procedure for synthesis of large areas of isolated VACNF arrays on Si substrates using the PECVD method with Ni catalysts. First, an n-type Si (1 0 0) substrate was cleaned thoroughly using "Radio Corporation of America" (RCA) I and II procedures. This was followed by a subsequent 10% HF dip for 30 s to remove the native oxide. After the HF dip, a layer of 200 nm photoresist (Ultra-i 123) was quickly spin-coated on the Si wafer. Next, the wafer was baked at 90 °C for 90 s. The photoresist was then patterned using a Lloyd's mirror type IL set-up with a He–Cd laser source (λ = 325 nm). The creation of periodic square patterns in the photoresist was achieved by two perpendicular exposures of 200 s each. The unexposed photoresist was etched away using the Shipley Microposit MF CD-26 developer and a circular-shape photoresist dot array on the Si wafer surface was left behind, as shown schematically in Fig. 2A. The samples were then subjected to an oxygen plasma etching process (power of 30 W, oxygen pressure of 0.5 mbar, and etching time of 30–120 s) to (i) remove the residual unexposed photoresist at the Si surface, and (ii) to trim the size of the photoresist dots. The second step controls the catalyst diameter and thus the CNF diameters.

Next, a 20 nm thick Cr was evaporated on the entire sample using an e-beam evaporator. The Cr layer on top of the photoresist was removed by lifting-off the photoresist. The photoresist lift-off and KOH anisotropic etching of the Si were achieved simultaneously by dipping the sample in 30% (by weight) KOH solution at 50 °C for around 300 s. Underneath the Cr holes which served as an etching hard mask, 4-fold symmetric arrays of inverted pyramids were produced, as seen in Fig. 2B. We then made use of the Cr holes as a deposition mask to evaporate a 10 nm silicon oxide layer and a 30 nm Ni film (at a base pressure of 10^{-6} Torr) onto the patterned sample to achieve, within the pyramids, an oxide layer that was sandwiched between the silicon substrate and the Ni film. The oxide layer is essential as a diffusion barrier to prevent silicidation between Ni and the Si substrate during the growth of CNFs. Finally, the Cr, the oxide and Ni layers above were lifted-off using the Chromium Cermet Etchant to reveal nano Ni pyramids sitting in the center of the silicon inverted pyramid arrays (Fig. 2C). The period for the inverted pyramid pattern was 500 nm and the "Ni pyramid" was around 200 nm in size. Note that with our patterning technique, the Ni catalysts are different from the usual spherical-shape catalysts commonly reported in the literature.

2.2. VACNFs growth

The Ni pyramid samples were then used for the growth of large area arrays of isolated VACNF, as shown in Fig. 2D, synthesized using the PECVD technique. The CNFs growth was performed at 700 °C at a pressure of 7.5 mbar in a 5:1 mixture of NH_3 and C_2H_2 (NH_3: 50 sccm and C_2H_2: 10 sccm). We controlled the CNFs length by varying the supply duration of the NH_3 and C_2H_2 in the PECVD system. Note that in the inset of Fig. 2D, the contour of the original pyramid has become rounded. This is a consequence of the etching of silicon by the gas mixture and the deposition a layer of amorphous carbon (confirmed using energy dispersive X-ray spectroscopy (EDX)) on the Si substrate during the CNFs growth. The amorphous carbon layer links the CNFs with the substrate and facilitates current flow for the field emission testing. The Ni pyramid enables us to grow mostly single CNF from a catalyst size up to 200 nm.

It is necessary to point out here that the unique shape of the Ni pyramid catalyst gives rise to the intriguing observation of a separation of top and bottom Ni catalysts in our CNFs growth, which is crucial in obtaining the very sharp-tipped CNFs, as shown in Fig. 2E. We have carried out EDX experiments on the CNFs and found a strong signal for Ni at the bottom of the CNFs, indicating the presence of bottom Ni catalysts. We have also demonstrated in HRTEM experiments (see Fig. 2F) the existence of Ni particles at the top of the

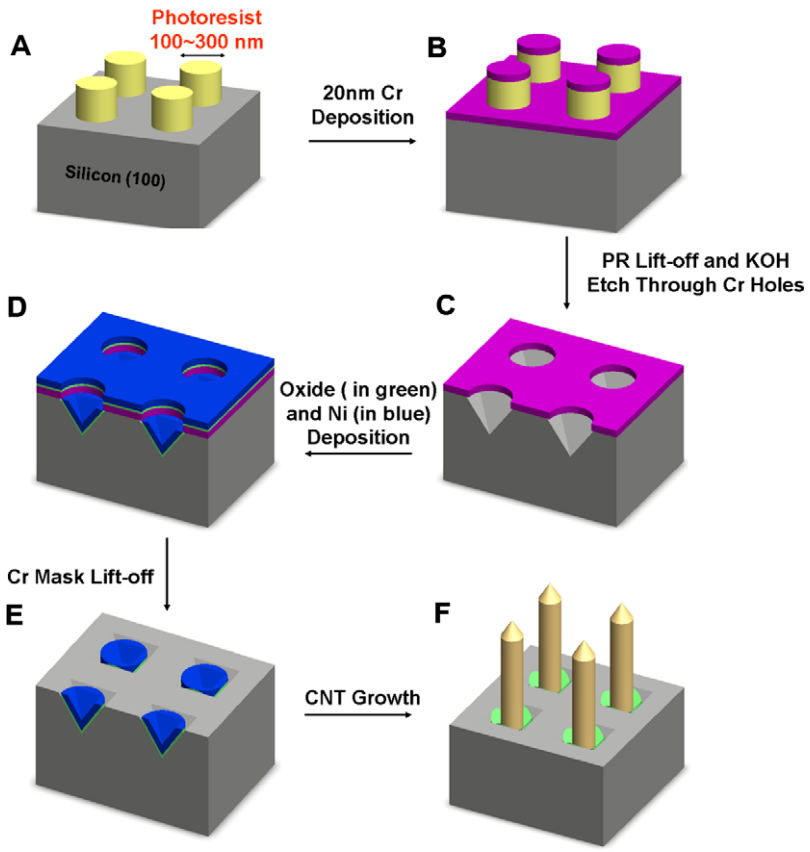

Fig. 1 – Process flow to synthesize arrays of isolated vertically-aligned carbon nanofibers (VACNFs) using Ni nanoparticles as catalysts.

CNFs. The HRTEM results also showed that our CNFs were amorphous in nature.

The ultra sharp tips are synthesized by purposely keeping the heater and DC plasma on for another 10 min after shutting off the C_2H_2 supply. We will be reporting, in a future publication, a systemic study of the creation of top and bottom Ni catalysts unique with our present method, and the influence of the PECVD growth conditions on the production of CNFs with very sharp tips.

3. Results and discussion

In field emission studies of CNTs, the field emission enhancement factor (β) is generally used to characterize the field emitter efficiency. From a simple electrostatic model, the enhancement factor for a single CNF or CNT, β_{single}, can be estimated from the geometry [14] of the emitters:

$$\beta_{single} = \beta_{tip} \times \alpha \quad (1)$$

where β_{tip} is the extra localized field enhancement from the upper tip of the CNF, and will be quite different for different tip shapes (open tip [15,16], sharper tip [17] or cone-shaped tip [18]), and α.

When considering the screening effects of CNTs, Γ is often used. Hence, β will be:

$$\beta = \frac{\beta_{single}}{\text{screening effect}} = \beta_{tip} \times \alpha \times \Gamma \quad (2)$$

In the present study, to investigate the influence of Γ and α on β, two sets of samples were synthesized with D fixed at 1.1 μm but with r = 100 and 200 nm, as shown in Fig. 3. In each set of samples, by controlling the growth time, CNFs of different l of ~0.55, 1.1 and 2.2 μm were obtained, and thus provided sets of samples with Γ = 2, 1 and 0.5. The values of α for samples in Set I (r = 200 nm) was half of that of the samples in the same row in Set II (r = 100 nm) in Fig. 3. The field emission tests were carried out using two parallel electrode plates setup in an ultrahigh vacuum chamber at a pressure of 1.1×10^{-9} Torr. The emission current (I) versus the applied voltage (V) for the two sets of VACNF samples are shown in Fig. 4A and B. The curves are relatively smooth and reproducible. The turn-on voltage was defined when $I = 1.0 \times 10^{-8}$ A (or at a current density of 5×10^{-4} mA/cm^2). The Fowler–Nordheim model was used to analyze the I–V characteristics of the two sample sets by re-plotting the I–V data as $\ln(I/V^2)$ versus $1/V$, as shown in Fig. 4C and D. From the slopes of each curve, and assuming a CNF work function of 5 eV [4], β was computed for each curve ($\beta = -\frac{b\phi^{3/2}d}{k}$, $\phi = 5$ eV, $b = 6.83 \times 10^9$ V eV$^{3/2}$ m^{-1}, d is the spacer thickness between CNF sample and anode, k is the slope from the fitting of the Fowler–Nordheim plots).

Firstly, we consider the influence of Γ on the value of β. For CNFs with a fixed radius r, when fibers are short, the screening of the electric field among CNFs will be negligible. As l increases, the field suppression among CNFs increases and thus

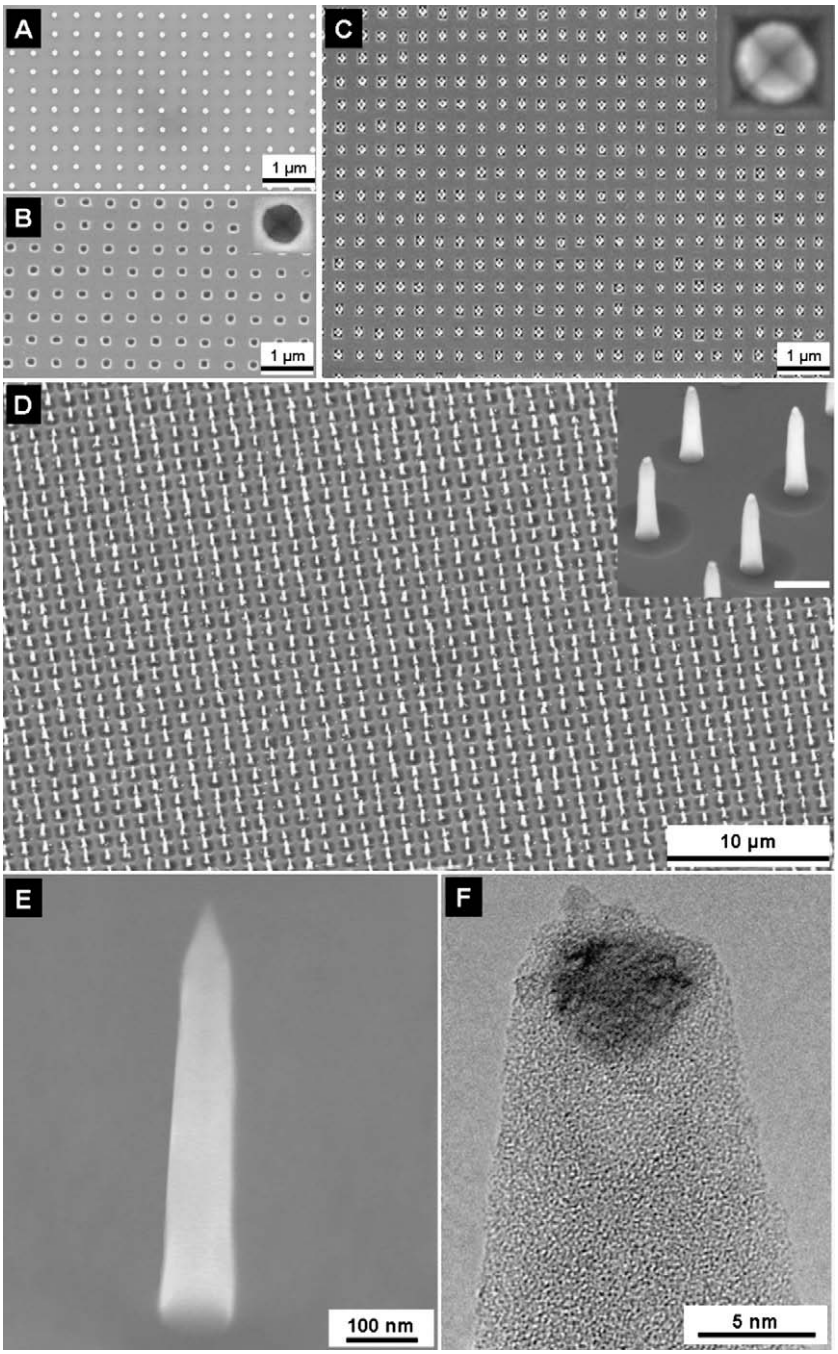

Fig. 2 – Scanning-electron-micrographs (SEM) of: (A) 200 nm diameter photoresist dots arrayed with a period of 450 nm. (B) Anisotropically etched Si (1 0 0) inverted pyramids undercutting the Cr holes with the inset showing a magnified view of a Cr hole. (C) Ni nano pyramids at the center of Si inverted pyramids after lift-off of Cr with the inset showing a magnified view of a Ni pyramid. (D) A large area of ordered VACNF arrays. The diameter of each CNF was ~200 nm, the length was ~1 μm, and the interfiber distance was 1.1 μm (45° Tilt). The inset is a magnified view of VACNF array with a scale bar of 500 nm. (E) One CNF with a diameter of 100 nm and 1.1 μm in length (45° Tilt). (F) High resolution transmission electron micrograph (HRTEM) of a CNF sharp tip (size less than 8 nm). The black dot on top is a Ni catalyst. The dimension of insets in (B) and (C) were 250 by 250 nm.

reduces the β value. Secondly, for fixed l, when r reduced, the value of D slightly increased. Thus, the field suppression among CNFs slightly reduced and β values increased. Hence, the screening effect is inversely proportional to Γ, and reducing l or r will reduce the screening effect and increase the value of β. Next we consider the role of α on the β value. Firstly, with r fixed, when fibers are short, the CNFs do not protrude from the surface significantly and therefore do not enhance the electric field effectively. As l increased, field emission is substantially enhanced through the CNFs, and the value of

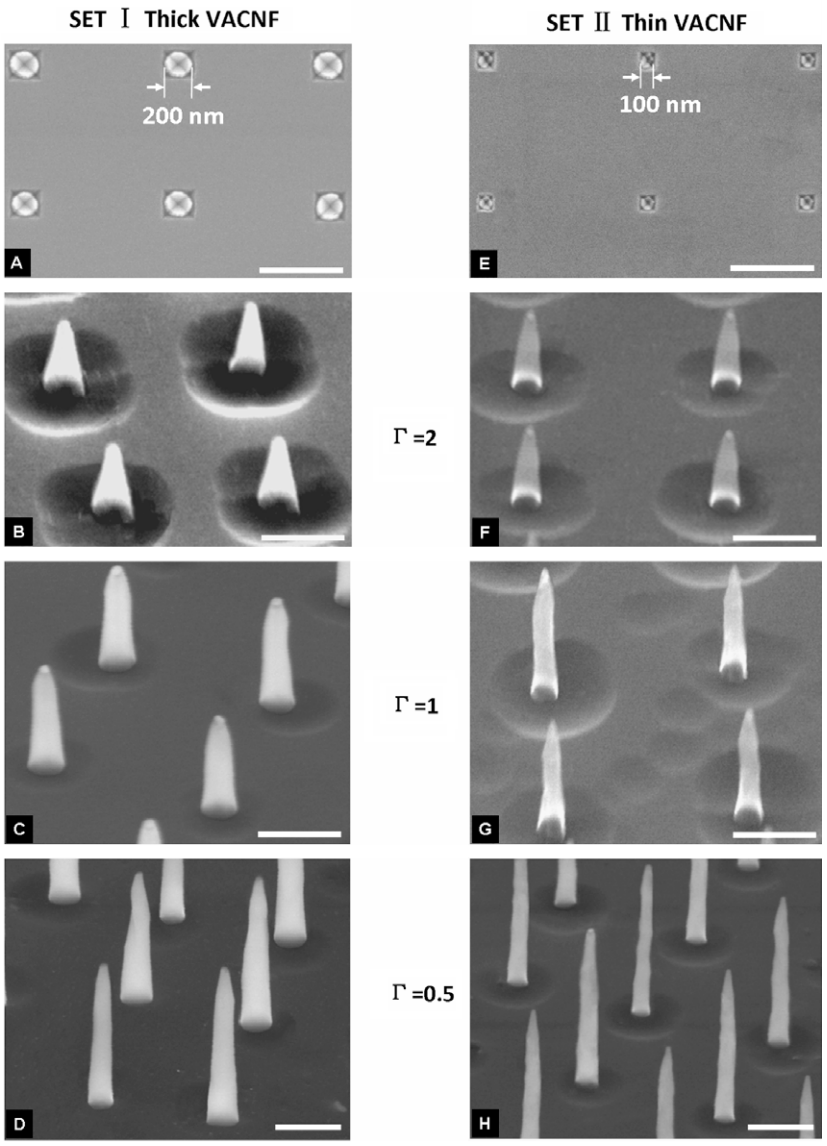

Fig. 3 – SEM images of patterned Ni catalyst arrays (A) and (E) and VACNF arrays (B–D, F–H) presenting (left) Set I (200 nm Ni catalysts) and (right) Set II (100 nm Ni catalysts). The period of the array is 1.1 μm. The CNFs lengths are of 0.55, 1.1 and 2.2 μm going from the top to bottom of the figure. Note that the VACNF arrays were viewed at a 45° tilted in the SEM. The scale bar in all pictures is 500 nm.

β increased significantly. Further increasing l would yield a diminishing increase of β value. Nevertheless, the β value is always proportional to l. Secondly, with fixed l, when r reduced, further electric field enhancement through the emitter and increased β value was found. Hence, we find that the β value is inversely proportional to r. Since $\alpha = l/r$, β is directly proportional to α.

Eq. (2) indicates that the β value depends on both Γ and α. Firstly, with r fixed, when CNFs were relatively short (i.e. in region A), the screening effect was insignificant and increasing l would significantly increase the β value. Hence, α is the dominant factor when l is small. When CNFs are relatively long (i.e. l is large, in region B), Γ will decrease and α will increase at a diminishing rate as l increases. This means that the screening effect gradually became more dominant and reduced the β value. The different dominating mechanisms that are responsible for the variation in β values in regions A and B and give rise to a maximum β value at $\Gamma = 1$. Secondly, with fixed l, when r reduces, the screening effect is slightly reduced and α increased, both of which increase the β value. This is in agreement with data shown in Fig. 5 that indicate that for a fixed Γ value, the CNFs with smaller r always have a higher β value.

We now compare our results to those published in the literature. For the samples prepared by the Teo et al. [4], the Γ value of VACNTs or VACNFs was fixed at two, which they indicated was in agreement with the prediction of Nilsson et al. [9]. However, no systematic study of the effects of α or Γ on β was carried out to validate the theoretical prediction. Suh et al. performed field emission studies on CNTs with different values of Γ and α. They demonstrated that the maximum value of β was obtained when Γ equals to one, and a higher α resulted in a higher value of β [7,8]. The first conclusion of Suh

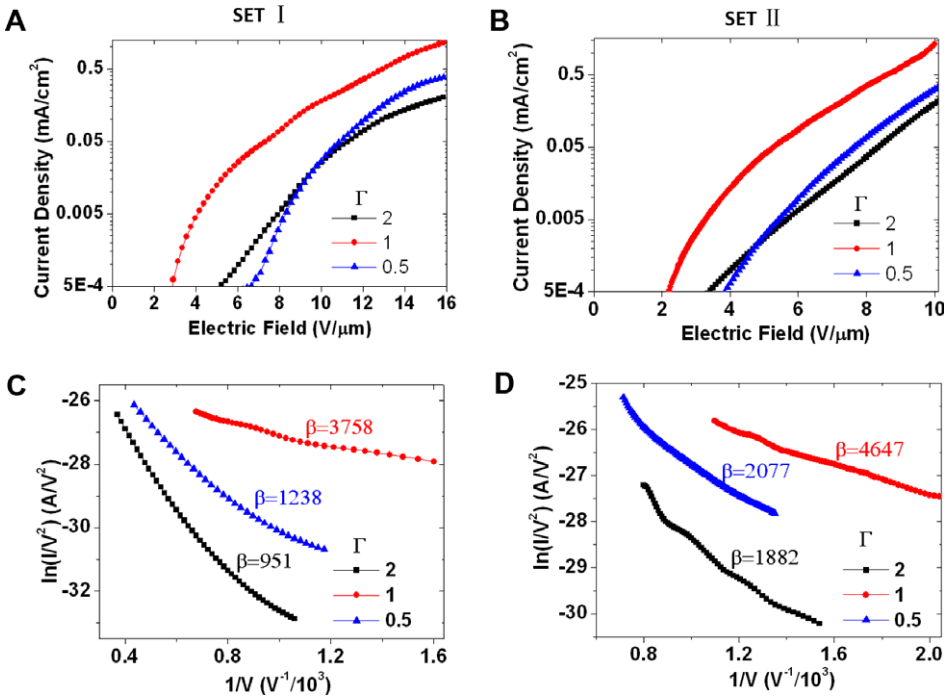

Fig. 4 – (A) Current–voltage (*I–V*) curve for the set of large-diameter VACNFs (~200 nm in diameter). (B) Current–voltage (*I–V*) curve for the set of VACNFs with small diameters (~100 nm in diameter). (C) Fowler–Nordheim plots for the large-diameter (200 nm) VACNF set. (D) Fowler–Nordheim plots for the small-diameter (100 nm) VACNF set.

et al. contrasts with the prediction of Nilsson et al. but is in good agreement with our present results. One possible reason for this discrepancy might be due to the fact that the aspect ratio in Nilsson's work was fixed at 500 (2 nm in diameter and 1 μm in length), while the aspect ratios in the present work and that of Suh et al. were much smaller (3–20). Nilsson et al. did not simulate the field emission characteristics of CNFs in the low-aspect-ratio regime, and therefore only considered one dominant factor, the screening effect. The second

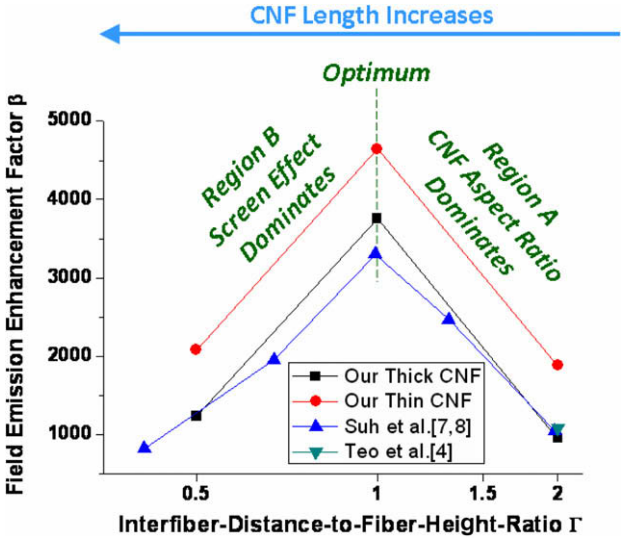

Fig. 5 – Plots of β versus Γ of our samples used in this work. Also shown in this figure are the results form Suh et al. [7,8] and Teo et al. [4].

conclusion of Suh et al., that higher values of α resulted in a higher values of β is complicated by the fact that the spacing between their CNFs was also changed.

A notable feature of our work is that the experimental results are in good agreement with that of Suh et al., despite the fact that very different patterning techniques and geometry parameters were used in the fiber growth in the two studies. This suggests that the value of β is mostly fixed by the value of Γ and α.

Henzie et al. [19] have also obtained Ni pyramids using a method very similar to our technique. They have employed a phase-shift technique for the patterning of the photoresist. In principle, the technique of Henzie et al. can also be used in the synthesis of VACNFs following our PECVD recipe. It should be noted, however, different masks are required to change catalyst size and period, which leads to a more costly process.

We have carried out some preliminary experiments on the reliability of CNF samples mentioned in the previous paragraphs. The CNF samples were placed inside the field emission chamber under ultra-high vacumm (~10^{-9} Torr) at a fixed electric field and tested for 24 h. Generally, all the CNFs survived such testing conditions with a relatively stable current density under prolonged period of testing. For example, we have tested a set of CNFs with 200 nm in diameter at the prescribed conditions with an electric field of 1 V/μm, the current density remained stable at 0.1 mA/cm^2 for 24 h.

4. Conclusions

We have developed a catalyst patterning method using IL to produce large area VACNFs with good control of the fiber's

diameter, spacing, length and tip sharpness. We have systematically studied the influence of the Γ and α on β and found that the optimum condition occurs when $\Gamma = 1$. This is consistent with other experimental data in the literature, but at variance with theoretical predictions.

Acknowledgments

The authors would like to thank Mr. Koo Chee Keong for his help to contact field emission test and EDX experiment. This work was partially supported by a grant from the Singapore-MIT Alliance. YJ would would like to thank the Singapore-MIT Alliance for the provision of a fellowship, WR and ZM would like to thank the National University of Singapore for the provision of research scholarships.

REFERENCES

[1] Fan S, Chapline MG, Franklin NM, Tombler TW, Cassell AM, Dai H. Self-oriented regular arrays of carbon nanotubes and their field emission properties. Science 1999;283:512–4.
[2] Treacy MMJ, Ebbesen TW, Gibson JM. Exceptionally high Young's modulus observed for individual carbon nanotubes. Nature (London) 1996;381:678–80.
[3] Chhowalla M, Teo KBK, Ducati C, Rupesinghe NL, Amaratunga GAJ, Ferrari AC, et al. Growth process conditions of vertically aligned carbon nanotubes using plasma enhanced chemical vapor deposition. J Appl Phys 2001;90:5308–17.
[4] Teo KBK, Chhowalla M, Amaratunga GAJ, Milne WI, Pirio G, Legagneux P, et al. Field emission from dense, sparse and patterned arrays of carbon nanotubes. Appl Phys Lett 2002;80:2011–3.
[5] Park KH, Lee S, Koh KH, Lacerda R, Teo KBK, Milne WI. Advanced nanosphere lithography for the areal-density variation of periodic arrays of vertically aligned carbon nanofibers. J Appl Phys 2005;97:024311–4.
[6] Vieria SMC, Teo KBK, Milne WI, Groning O, Gangloff L, Minoux E, et al. Investigation of field emission properties of carbon nanotube arrays defined using nanoimprint lithography. Appl Phys Lett 2006;89:022111–3.
[7] Suh JS, Jeong KS, Lee JS, Han I. Study of the field-screening effect of highly ordered carbon nanotube arrays. Appl Phys Lett 2002;80:2392–4.
[8] Yoon SM, Chae J, Suh JS. Comparison of the field emissions between highly ordered carbon nanotubes with closed and open tips. Appl Phys Lett 2004;84:825–7.
[9] Nilsson L, Groening O, Emmenegger C, Kuettel O, Schaller E, Schlapbach L, et al. Scanning field emission from patterned carbon nanotube films. Appl Phys Lett 2000;76:2071–3.
[10] Smith RC, Silva SRP. Maximizing the electron field emission performance of carbon nanotube arrays. Appl Phys Lett 2009;94:133104–6.
[11] Choi WK, Liew TH, Chew HG, Zheng F, Thompson CV, Wang Y, et al. A combined top-down and bottom-up approach for precise placement of metal nanoparticles on silicon. Small 2008;4:330–3.
[12] Walsh M. On the design of lithographic interferometers and their applications. PhD thesis. 77 Massachusetts Avenue, Cambridge, MA, USA: Massachusetts Institute of Technology; 2004.
[13] Geirmann AL, Thompson CV. Solid-state dewetting for ordered arrays of crystallographically oriented metal particles. Appl Phys Lett 2005;86:121903–5.
[14] Chen XH, Chang YQ, Wang Z, Yu DP. Effect of ion beam etching on the field emission of carbon nanotube arrays. Solid State Commun 2009;149:523–6.
[15] Rinzler AG, Hafner JH, Nikolaev P, Lon L, Kim SG, Tomanek D, et al. Unraveling nanotubes: field emission from an atomic wire. Science 1995;269:1550–3.
[16] Tsai SH, Chao CW, Lee CL, Shih HC. Bias-enhanced nucleation and growth of the aligned carbon nanotubes with open ends under microwave plasma synthesis. Appl Phys Lett 1999;74:3462–4.
[17] Cumings J, Collins PG, Zettl A. Materials: peeling and sharpening multiwall nanotubes. Nature 2000;406:2586.
[18] Merkulov VI, Guillorn MA, Lowndes DH, Simpson ML, Voelkl E. Shaping carbon nanostructures by controlling the synthesis process. Appl Phys Lett 2001;79:1178–81.
[19] Henzie J, Kwak ES, Odom TW. Mesoscale metallic pyramids with nanoscale tips. Nano Lett 2005;5:1199–202.